Article

Not peer-reviewed version

Adaptive Variable Design Algorithm for Improving Topology Optimization in Additive Manufacturing

Abraham Vadillo Morillas *, Jesús Meneses Alonso, Alejandro Bustos Caballero, Cristina Castejon Sisamón, Alessandro Ceruti

Posted Date: 4 June 2024

doi: 10.20944/preprints202406.0077.v1

Keywords: topology optimization; optimization software; performance optimization; manufacturability; discreteness

Preprints.org (www.preprints.org) | NOT PEER-REVIEWED | Posted: 4 June 2024 doi:10.20944/preprints202406.0077.v1

Article

Adaptive Variable Design Algorithm for Improving Topology Optimization in Additive Manufacturing

Abraham Vadillo Morillas [1,*], Jesús Meneses Alonso [2], Alejandro Bustos Caballero [3], Cristina Castejón Sisamón [2] and Alessandro Ceruti [4]

[1] MAQLAB Research Group. Mechanical Engineering Department. University Carlos III de Madrid
[2] MAQLAB Research Group. Mechanical Engineering Department. University Carlos III de Madrid & Pedro Juan de Lastanosa Research Institute; meneses@ing.uc3m.es; castejon@ing.uc3m.es
[3] MAQLAB Research Group. Depaertment of Mechanics. Universidad Nacional de Educación a Distancia; albustos@ind.uned.es
[4] Industrial Engineering Department. University of Bologna.; alessandro.ceruti@unibo.it
* Correspondence: abvadill@ing.uc3m.es

Abstract: CAD-CAE software companies have introduced numerous tools aimed at facilitating topology optimization through Finite Element Simulation, thereby enhancing accessibility for designers via user-friendly interfaces. However, the imposition of intricate constraint conditions or additional restrictions during calculations may introduce instability into the resultant outcomes. In this paper, an algorithm for updating the design variables called Adaptive Variable Design is proposed to keep the final design space volume of the optimized part always under the target value while giving the main algorithm multiple chances to update the optimization parameters and search for a valid design. This algorithm aims to producing results that are more conducive to manufacturability and potentially more straightforward in interpretation. A comparison between several commercial software and the proposed algorithm, implemented in MATLAB, is carried out to prove the robustness of the latter. By simulating identical parts under similar conditions, we seek to generate comparable results and underscore the advantages stemming from the adoption and comprehension of the proposed topology optimization methodology. Our findings reveal that the integrated enhancements within MATLAB pertaining to the topology optimization process yield favourable outcomes with respect to discretization, and the manufacturability of resultant geometries. Furthermore, we assert that the methodology evaluated within MATLAB holds promise for potential integration into commercial packages, thereby enhancing the efficiency of topology optimization processes.

Keywords: topology optimization; optimization software; performance optimization; manufacturability; discreteness

1. Introduction

Topology optimization initially found its roots in addressing structural challenges through mathematical formulations, pioneered by Mitchell, Schmit and Dorn et al. [1–3]. However, its widespread adoption was not realized until the emergence of the Finite Element Method (FEM) and its application to engineering structures [4–7] (together with other later relevant advances for the application of FEM to structural optimization [8–10]), alongside the integration of optimization systems combining FEM and topology optimization, as in [11,12]. Subsequently, with the computerization of the methodology pioneered by Bendsøe and Kikuchi [13], topology optimization achieved maximum efficiency. Recent years have witnessed further advancements in topology optimization applications, notably with contributions from Sigmund [14].

These advancements have enabled companies specialized in structural simulation, commercial software, and CAD-CAE packages to integrate topology optimization into their products. Consequently, designers can now utilize this methodology without necessitating extensive knowledge of the underlying mathematics and physics involved in the calculation process. However,

doi:10.20944/preprints202406.0077.v1

despite the accessibility afforded by commercial software, certain limitations persist, particularly in terms of result interpretation and adherence to strict manufacturing constraints.

Several researchers have recently developed tools aimed at achieving better results, as evidenced by the works of Guest et al. [15], Andreassen et al. [16], Liu and Tovar [17], Schevenels and Sigmund [18], Pellens et al. [19], Langelaar [20,21], Fu et al. [22], and Lee et al. [23]. These tools have been tested and applied to real-world components in some instances. More recent studies and reviews evidence a trend to use and develop this method for future applications in the world of part design [24–30]

The paper conducts a comparative analysis on the structural optimization of a real part using four commercial software codes (PTC Creo Parametric 6.0.1.0, Altair HyperMesh 2023.1, Solidworks 2023, and Ansys Workbench 2023R1) and a self-implemented MATLAB code. The aim is to demonstrate the benefits of understanding and applying the core principles of the topology optimization process over the use of popular solvers, like Tosca, OptiStruct, Ansys, and PTC. While existing literature includes other comparative studies (Choi et al. [31], Dalpadulo et al. [32], Tyflopoulos et al. [33], and Struz et al.[34]), these primarily focus on identifying the best software for practical use and aiding designers in selecting suitable tools for their projects, without suggesting further improvements to standard commercial codes or proposing a general-purpose method.

In this study, multiple implementations in MATLAB are undertaken to enhance part optimization results, highlighting the development of an algorithm for updating the optimization parameters and, as a consequence, the design variables avoiding the use of robust formulation. We named it as Adaptive Variable Design (AVD). Furthermore, to validate the developments presented in this work, comparisons are made between the results obtained from the MATLAB implementations and those provided by commercial packages.

The comparison is facilitated through a case study which involves designing a racing motorcycle triple tree for fused deposition modelling (FDM). Identical loads, restrictions, and constraints are employed in all the commercial packages and MATLAB implementations. To prevent non-printable features in the result, Heaviside filters are used to derive a minimum length scale adapted to this specific case. Additionally, a new algorithm is introduced and explained that addresses convergence without requiring a robust formulation.

2. Case Study

The case study in this investigation involves the design of a racing motorcycle triple tree, specifically tailored for fused deposition modelling (FDM) manufacturing. The triple tree (highlighted in red in **Error! Reference source not found.**a) is a critical structural component that links the motorbike's front structure to the frame, facilitating steering. It undergoes significant loads during braking due to mass transfer and inertial forces which are transferred to the front wheel.

To identify the load conditions, a multi-body dynamics (MBD) analysis of a complete motorcycle model is conducted (**Error! Reference source not found.**a). This analysis considers the most limiting negative acceleration during braking. A dummy, positioned as a braking rider (**Error! Reference source not found.**b), is added to the MBD model since the rider's weight significantly affects the model's behaviour. The resultant acceleration is analysed to determine reaction forces in the triple tree. A small lateral load is also introduced to aid consistent shape generation. For static analysis in the topology optimization process, the triple tree is clamped in the direction of the axle hole restricting all degrees of freedom, with forces applied at the front fork holes (see Figure 2).

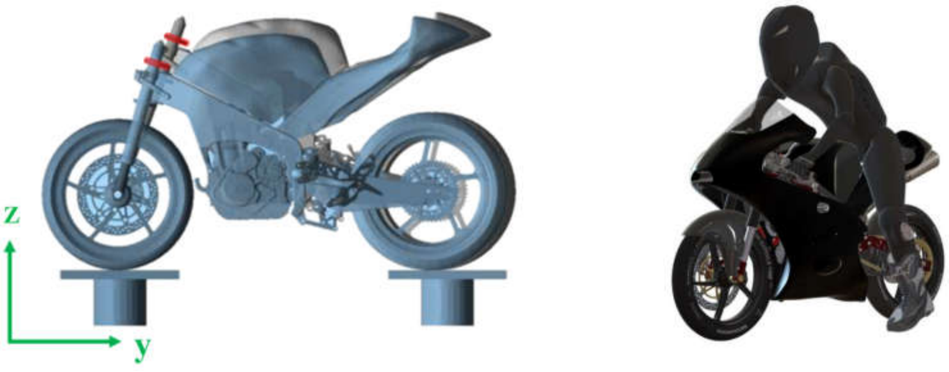

(**a**) (**b**)

Figure 1. (**a**) MBD analysis result of the braking test with the triple tree highlighted in red, (**b**) Rider in braking position utilized during the MBD analysis.

The primary objective of the optimization is to minimize the compliance of the part while adhering to a constraint that limits the final volume of the design space to below 30% of its original value. The design space is the volume where the design variables can be changed during the optimization process, i.e. the regions where the solver will change the shape**.** The design domain is represented in red in **Error! Reference source not found.**, while the non-design space is coloured in blue. Furthermore, manufacturing constraints are incorporated into all models, including:

- Minimum solid phase length of 2.4 mm: This constraint ensures that features smaller than 6 times the size of the extruded material are avoided, given the typical nozzle pick diameter of an FDM printer is 0.4 mm.
- Symmetry in the YZ plane: While forces are symmetrical with respect to this plane, ensuring symmetric results is essential for consistent behaviour and stiffness across both sides of the front fork. This plane is represented in green in **Error! Reference source not found.**.
- Extrusion in Z-direction: To maintain comparability across different software packages, an extrusion constraint is applied as a 90° overhang constraint. Although overhang angle is a common constraint in topology optimization for additive manufacturing, its implementation varies among software packages. In this case, the geometry of the part makes it suitable for this constraint due to its small thickness relative to other dimensions.

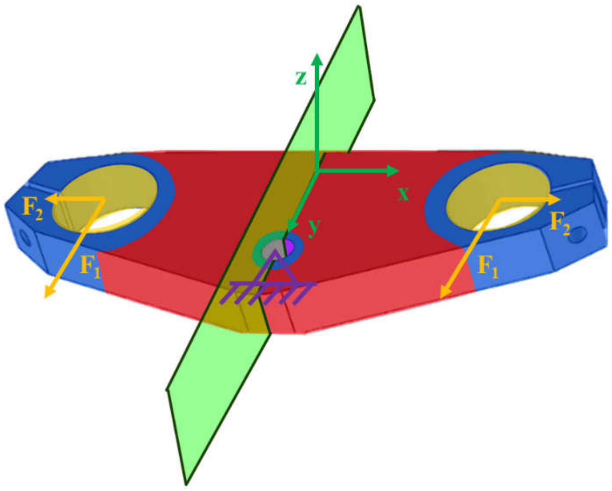

Figure 2. Motorcycle triple tree. In red the design space is represented, while the non-design space is in blue. The symmetry plane YZ is coloured green. The applied forces zones and directions are indicated in yellow, and the restricted areas are showcased in purple.

The mentioned loads F_1 and F_2 are 1500N and 250N respectively. These forces and the clamped direction axle are represented in yellow and purple in **Error! Reference source not found.**. The considered material is aluminium 7075T6, being its relevant mechanical properties the density $\rho = 2810Kg/m^3$, the Young modulus $E_0 = 72 \cdot 10^9 Pa$ and the Poisson ratio $\upsilon = 0.33$. The part limits are settled in a prismatic space of 288x102x25 mm. These values are used with all the cases in commercial software packages and MATLAB implementations.

Results are evaluated based on manufacturability and assessed using software to verify compliance with manufacturing constraints. Additionally, the interpretability of results is analysed, with a focus on the discreteness of the resultant density field. A more discrete density field (comprising only 0 and 1 densities) indicates lower interpretability of the result.

3. MATLAB Implementation

The MATLAB topology optimization process is applied using well-known working codes [16,17,35,36] as the core for the implementations. As mentioned before, the objective of all the cases is to minimize the compliance (i.e. minimize the global strain energy) of the design space while keeping its final volume under 30% of the original one. This can be expressed as in Equation 1:

$$\begin{gathered}\min \mathrm{c}(\rho) = \mathbf{U}^{\mathrm{T}}\mathbf{K}\mathbf{U} = \sum_{\mathrm{e}=1}^{\mathrm{N}} \mathrm{E}_{\mathrm{e}}(\rho_{\mathrm{e}})\mathbf{u}_{\mathrm{e}}^{\mathrm{T}}\mathbf{k}_0\mathbf{u}_{\mathrm{e}} \\ \text{subjected to: } \begin{cases} \mathrm{V}(\rho)/\mathrm{V}_0 \leq \mathrm{f} \\ \mathbf{KU} = \mathbf{F} \\ 0 \leq \rho_{\mathrm{i}} \leq 1 \end{cases}\end{gathered} \tag{1}$$

Where **K**, **U** and **F** are the global stiffness matrix and the global displacement and forces vectors, respectively; N is the total number of elements, $\mathbf{u}_{\mathrm{e}}$ is the e^{th} element displacement vector, $\mathbf{k}_0$ is the element stiffness matrix, ρ_{e} is the e^{th} element density, V_0 is the initial design volume and $\mathrm{V}(\rho)$ is the design volume, which can be described as presented in Equation 2; and f is the prescribed upper limit of the volume fraction constraint, settled to 0.3 for all the cases.

$$\mathrm{V}(\boldsymbol{\rho}) = \frac{\sum_{\mathrm{e}=1}^{\mathrm{n}} \rho_{\mathrm{e}}}{\mathrm{N}}, \qquad \mathrm{n} \in (1, \mathrm{N}) \tag{2}$$

The used optimization algorithm is the Optimality Criteria (OC) [37,38]. This algorithm is used for updating the design variables according to the objective and restrictions. Additionally, the linear density filter [39,40] with conic weights weighting technique is used for avoiding the checkerboard structures formation [41]. The optimization algorithm and density filter formulation can be found in the scientific literature [16,17,35,36].

3.1. Geometry and Design Space Implementation

To improve performance in terms of calculation time and result manufacturability compared to commercial software, a 2D analysis is implemented, followed by an extrusion to the final thickness of the part. Symmetry conditions, considering only half the part, are applied to meet the described conditions.

For defining the initial mesh, the limits of the part in millimetres are translated into elements, so the initial mesh is 144x102 elements long. The design domain consists of three different spaces: the design space, represented in red in **Error! Reference source not found.**; the non-design space, coloured in blue in **Error! Reference source not found.**; and the void space, showcased in green in **Error! Reference source not found.**. Active and passive elements [16,17] are used for defining the behaviour of each space, in a way that:

- Void space: The density ρ_{e} of the elements is always 0. It defines the shape of the initial design of the triple-tree and does not influence the structural calculations. It is formed by passive elements.

- Non-design space: It encompasses volumes that must remain the same at the end of the optimization process. The density ρ_e of the elements inside these volumes is always 1, and they do influence the structural calculations. It is constituted by active elements.
- Design space: The density of the elements ρ_e vary from 0 to 1 with intermediate values adhering to a density-based approach topology optimization. The volume constraint defined in Equation 2 is applied only to this space, as is the only space that can vary its design variables in every iteration.

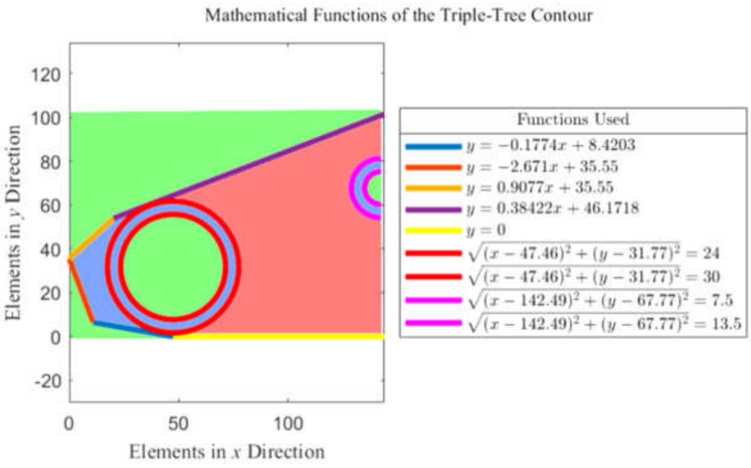

Figure 3. Mathematical functions of the triple-tree contour. The functions are written in the legend "Functions Used". In shaded green the void space is represented, in shaded red, the design space; and in shaded blue the non-design space.

3.2. Heaviside Step Function

Sigmund [42] introduced the morphology-based filters based on automatic inspection and restoration of image data [43]: the erode, dilate, close, open, close-open and open-close filters. These filters strive to maintain the beneficial features of density filters while preventing the grey transition from the void phase to the solid phase. In doing so, intermediate densities are reduced to yield a more binary result. This binary result manifests as a less interpretable shape because the displayed shape doesn't obscure elements with intermediate densities that significantly affect the structural calculations.

The use of the close-open filter is especially interesting in this case, as a minimum length of the solid phase can be obtained. This minimum length is defined by the radius of the density filter, which is set to 2.4 as stated in epigraph 0. If “∧” represents the dilation operator and “∨” the erosion operator, the close-open filter can be expressed as in Equation 3 [42]:

$$\hat{\check{\check{\hat{\rho}}}}_e = \hat{\check{\check{\hat{\rho}}}}_e\left(\check{\check{\hat{\rho}}}_{i\epsilon N_e}\left(\check{\hat{\rho}}_{j\epsilon N_i}\left(\hat{\rho}_{k\epsilon N_j}\left(\rho_{l\epsilon N_k}\right)\right)\right)\right) \tag{3}$$

In this case, the filter is applied to the design space, and e, i, j, k and l are the elements inside the design space, being $e \equiv i \equiv j \equiv k \equiv l$. The used morphology operator is the smooth Heaviside function proposed by Wang et al. [44] and shown in Equation 4. When $\eta = 1$, the operator behaves as a min operator (erode) if β approaches to ∞; and for $\eta = 0$, the operator behaves as a max operator (dilate) if β approaches to ∞. For β approaching zero, the operator behaves as the linear density filter with conic weights.

$$\bar{\rho}_e = \frac{\tanh(\beta\eta) + \tanh\left(\beta(\tilde{\rho}_e - \eta)\right)}{\tanh(\beta\eta) + \tanh\left(\beta(1 - \eta)\right)} \tag{4}$$

Where $\tilde{\rho}_e$ is the density field after the density filter, and $\bar{\rho}_e$ is the density field after the Heaviside filter. This expression can be derived for the calculation of sensitivities. This expression is shown in Equation 5:

$$\frac{\partial\bar{\rho}_e}{\partial\tilde{\rho}_e} = \beta\frac{\mathrm{sech}^2\left(\beta(\tilde{\rho}_e - \eta)\right)}{\tanh\beta + \tanh\left(\beta(1-\eta)\right)} \tag{5}$$

Combining Equations 3 and 5 through a chain rule, the sensitivities of the density field $\partial\hat{\check{\check{\hat{\rho}}}}_e/\partial\rho_e$ can be calculated as in Equation 6:

$$\frac{\partial\hat{\check{\check{\hat{\rho}}}}_e}{\partial\rho_e} = \frac{\partial\hat{\check{\check{\hat{\rho}}}}_e}{\partial\check{\check{\hat{\rho}}}_e}\frac{\partial\check{\check{\hat{\rho}}}_e}{\partial\check{\hat{\rho}}_e}\frac{\partial\check{\hat{\rho}}_e}{\partial\hat{\rho}_e}\frac{\partial\hat{\rho}_e}{\partial\tilde{\rho}_e}\frac{\partial\tilde{\rho}_e}{\partial\rho_e} \tag{6}$$

The discreteness is analysed with the formula presented by Sigmund [42] in Equation 7 known as measure of non-discreteness:

$$\mathrm{M}_{\mathrm{nd}} = \frac{\sum_{e=1}^{N} 4\,\hat{\check{\check{\hat{\rho}}}}_e(1-\hat{\check{\check{\hat{\rho}}}}_e)}{N} \times\ 100\% \tag{7}$$

As the result becomes more discrete (binary, or 0-1), M_{nd} will approach 0; while a density field formed solely by intermediate densities of 0.5 will yield a result of 100.

3.3. Parameters Update Algorithm

The addition of new constraints and filters to the optimization algorithm makes convergence more difficult due to the numerous conditions the final design must meet and the limited design parameters available for modification in the end stages of the optimization. While the Heaviside step function with the morphology-based filter helps trend the design towards binary densities, the move limit at each step of the OC routine is often smaller than the density difference between a low-density and high-density element in the final optimization phase. This means that major changes are not done in the OC routine, and more intermediate densities are needed. Similar issues arise with other optimization algorithms, such as sequential quadratic programming or the method of moving asymptotes, that usually use smooth constraints to obtain convergence [45].

Some authors address the issue using robust formulation, that employs the worst-case scenario for each feature of the optimization problem (e.g. an eroded design for compliance, or a dilated design for volume constraint) [46–50]. However, this often results in a mathematically correct result, yet impractical outcomes for designs oriented towards manufacturing of real parts. In this paper, the algorithm AVD is proposed to keep the final design space volume always under the target value while giving the main algorithm multiple chances to update the design variables and search for a valid design. This algorithm should result in not fully discrete designs, but with a M_{nd} between 0 and 5%, which won't affect the final interpretation of the optimization result.

First, the parameter β increases by 1.2 every 25 iterations only if the M_{nd} is larger than the prescribed $\mathrm{M}_{\mathrm{nd}}^{\mathrm{ref}}$, which is initially set to 1 (although it can be changed within the algorithm). These changes are explained later in this epigraph. The penalization p follows a similar continuations scheme, starting at 2 and increasing by 1.01 up to a maximum value of 6.

The rest of the algorithm, where the filter parameters are modified to find an appropriate convergence, works as in the flowchart presented in **Error! Reference source not found.**:

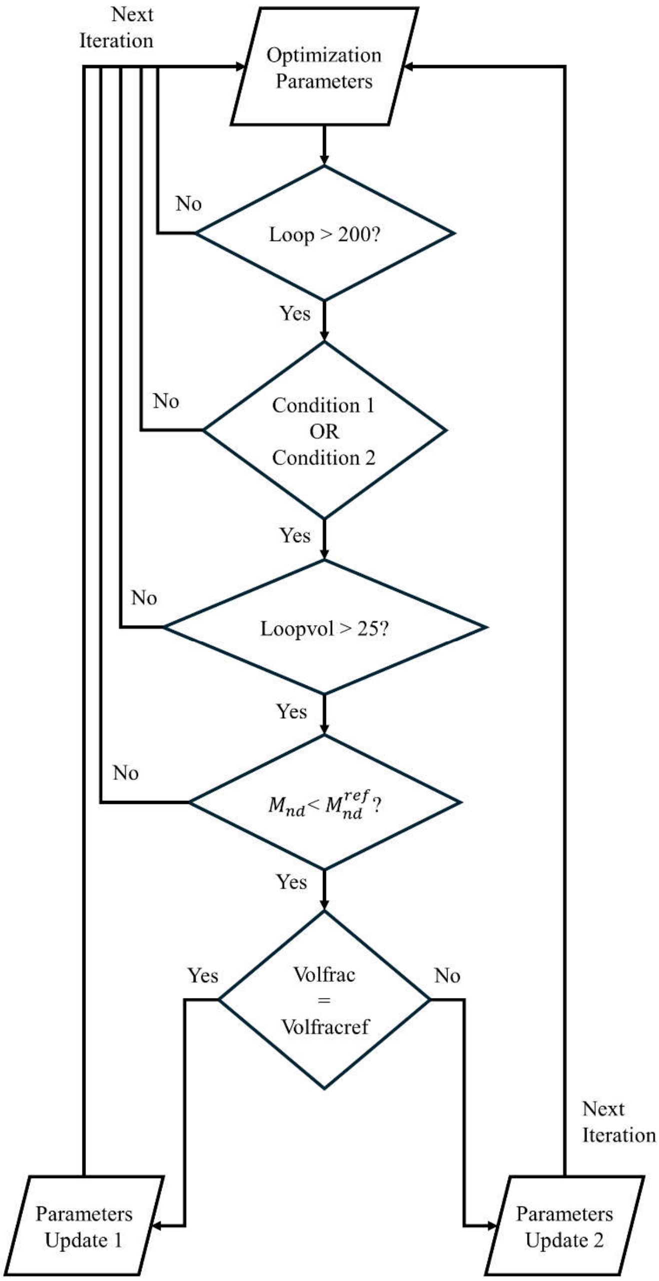

Figure 4. Flowchart of the design variables update algorithm.

Where:

- The algorithm begins operation in the 201st iteration, allowing the algorithm to create an initial design.
- Condition 1 compares the maximum density change of the last 50 iterations. If the median value is near the maximum permitted change, the condition is satisfied. It can be expressed as in Equation 8:

$$\overline{\mathrm{ch}(\mathrm{loop}-49\!:\mathrm{loop})} \geq \mathrm{move}-0.05 \tag{8}$$

Where ch is the maximum density change in every iteration, loop is the iteration number and move is the target value for maximum permitted change in every iteration.

- Condition 2 compares the same change value of the last 50 with the last 100 iterations. If the median change in both scenarios is similar, the condition is satisfied. It can be expressed as in Equation 9:

$$1.05 \geq \overline{ch(loop-49:loop)}/\overline{ch(loop-99:loop)} \geq 0.95 \qquad (9)$$

- Loopvol is a counter that prevents consecutive parameter updates. It is restarted when the parameters are updated and must surpass 25 for the next parameters update.
- M_{nd} must stay under 1 to maintain a relatively high discreteness.
- Volfrac is the actual iteration volume fraction following Equation 2.
- Volfracref is the prescribed volfrac upper limit described in Equation 1.
- In Parameters Update 1, the parameter β is set to 1, and a new parameter "Volfracobj" is introduced. Volfracobj is the value that Volfrac takes as a reference for the OC routine when Parameters Update 1 is activated. Initially matching Voldracref, it reduces Volfracobj whenever Parameters Update 1 is active until reaching a minimum of Voldracref-0.05. Additionally, all the loop counter variables are restarted and the $\mathrm{M}_{\mathrm{nd}}^{\mathrm{ref}}$ is also restarted to a value of 1.
- In Parameters Update 2, Volfrac is expanded by 0.005. Note that this update occurs when Volfrac<Volfracref, so Volfrac increases until matching Volfracref, thereby triggering Parameters Update 1 instead of Parameters Update 2. Additionally, the $\mathrm{M}_{\mathrm{nd}}^{\mathrm{ref}}$ is expanded by 0.5 and the parameter β is halved.

4. Software Packages Configuration

The setup of each software for addressing the optimization and geometry constraints explained in Epigraph 0 is summarized next in **Error! Reference source not found.** for the sake of clarity and reproducibility. As the density-based topology optimization is a mesh-dependant method, information about the mesh and the simulation times are also provided.

Table 1. Sofware package's configuration.

Software	Mesh Information	Objective	Constraints	Geom. Restrictions	Sim.Time (HH:mm:ss)
HyperMesh 2023.1	491809 CTETRA elements. Mesh size = 2.5.	Minimize compliance.	Volumefrac upper limit = 0.3.	Mindim = 2.4. Pattern grouping = 1 pln sym. No twist extrusion.	00:29:29
Parametric 6.0.1.0	433488 Tetrahedrons. Mesh size = 1.98 mm.	Minimize strain energy.	Mass fraction upper limit 0.3.	Extrude along Z axis. Mirror about YZ plane. Minimum member size = 2.4.	00:25:45
SolidWorks 2023	Default mesh 2 mm size. 349368 elements	Best stiffness-to-weight ratio.	70% mass reduction.	Thickness control – min = 4 mm. Symmetry control. De-mold direction – Stamping (pull direction only).	00:59:12
Workbench 2023 R1	467009 Tetrahedrons. Mesh size = 2.2 mm.	Minimize compliance.	Volume constraint – 30% retain.	Member size – Min Size = 2.4 mm. Symmetry design constraint. Extrusion.	00:52:57

The thickness control in SolidWorks is adjusted to 4 mm instead of 2.4 mm due to a software restriction: minimum thickness must be twice the mesh size. For a 2.4 mm minimum thickness, the resulting mesh would be too large to compute.

All programs are configured to perform density-based topology optimization with SIMP as a weighting scheme, along with default parameters for the solver and the SIMP itself. Further information can be found in the developers' documentation [51–55].

5. Results

The resultant density fields are compared by representing three different density thresholds to evaluate the discreteness of the different results. **Error! Reference source not found.** illustrates the resulting density fields, where elements with a density $\rho_e > 0.1$ are represented in blue, elements with a density $\rho_e > 0.5$ are depicted in green; and in red, elements with a density $\rho_e > 0.9$ are represented.

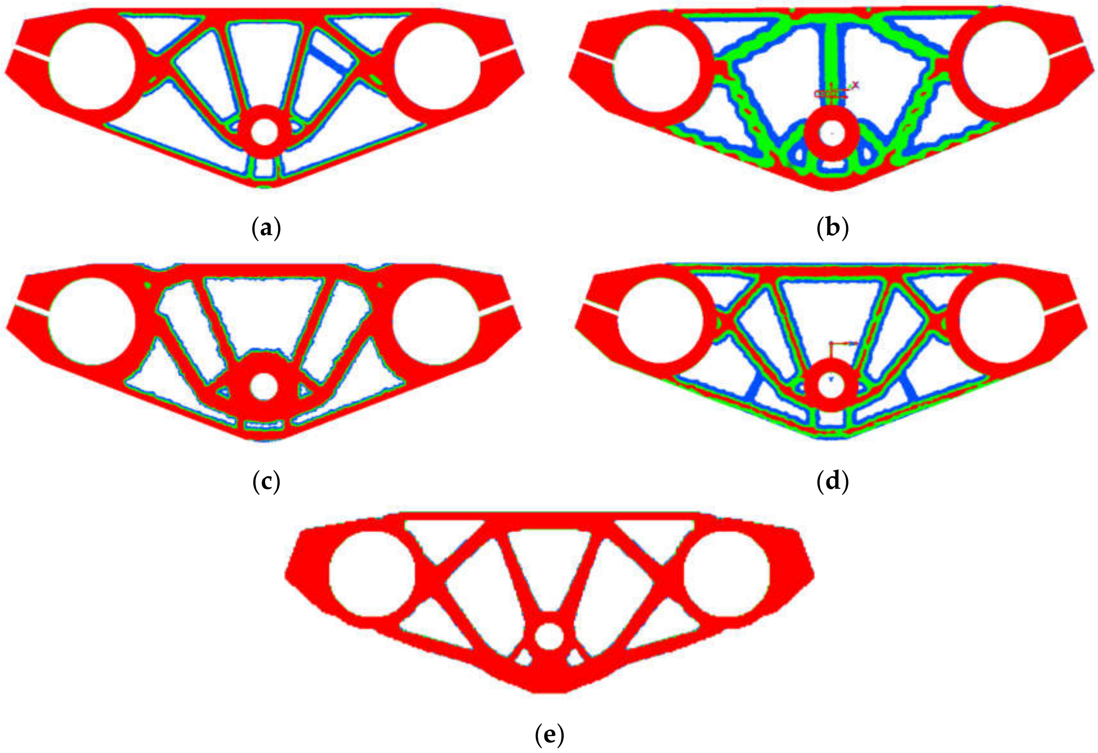

(**a**) (**b**)

(**c**) (**d**)

(**e**)

Figure 5. Results of the topology optimization process with the software packages and. the MATLAB implementations. Coloured in blue, elements with a density over 0.1 are represented; in green, elements with a density over 0.5; and in red, elements with a density over 0.9. (**a**) HyperMesh 2023.1 (**b**) CREO Parametric 6.0.1.0. (**c**) SolidWroks 2023 (**d**) ANSYS Workbench 2023 R1 (**e**) MATLAB.

The numerical results and comments regarding the resulting shapes and density fields are summarized next in **Error! Reference source not found.**.

Table 2. Results summary.

Software	Volume Fraction	Max. Displacement	Advantages	Disadvantages
HyperMesh 2023.1	31.956%	$4.055\cdot10^{-2}$ mm	Accurate with objective and constraints. Good discreteness.	Symmetry constraint violated in low densities. Slight volume fraction constraint violation.
CREO Parametric 6.0.1.0	36.475%	$3.825\cdot10^{-2}$ mm	Well defined and simple shape.	General instabilities in result. Lack of high-density elements.

				Volume fraction constraint violation.
SolidWorks 2023	46.117%	3.529·10^{-2} mm	Best discreteness in software packages	High volume fraction constraint violation. Low density features.
ANSYS Workbench 2023 R1	35.929%	3.629·10^{-2} mm	Best calculation performance in software packages.	Volume fraction constraint violation. Lack of continuity in high density range.
MATLAB	29.540%	4.674·10^{-2} mm	Quasi binary result (M_{nd}=1.386) Didn't violate volume fraction constraint. Simulation time significantly lower: 00:03:02	Harder geometry introduction to the algorithm. Improve mesh definition, which would increase calculation time.

The optimization outcomes are interpreted into CAD designs with a density threshold of 0.5, and subsequently examined with a Slicer software for FDM, Ultimaker Cura 5.4.0. In **Error! Reference source not found.** the CAD interpretations done in SolidWorks 2023 and the manufacturing analyses performed in Cura 5.4.0 are showcased, with red arrows pointing to the critical features where the minimum length constraint has been invoked.

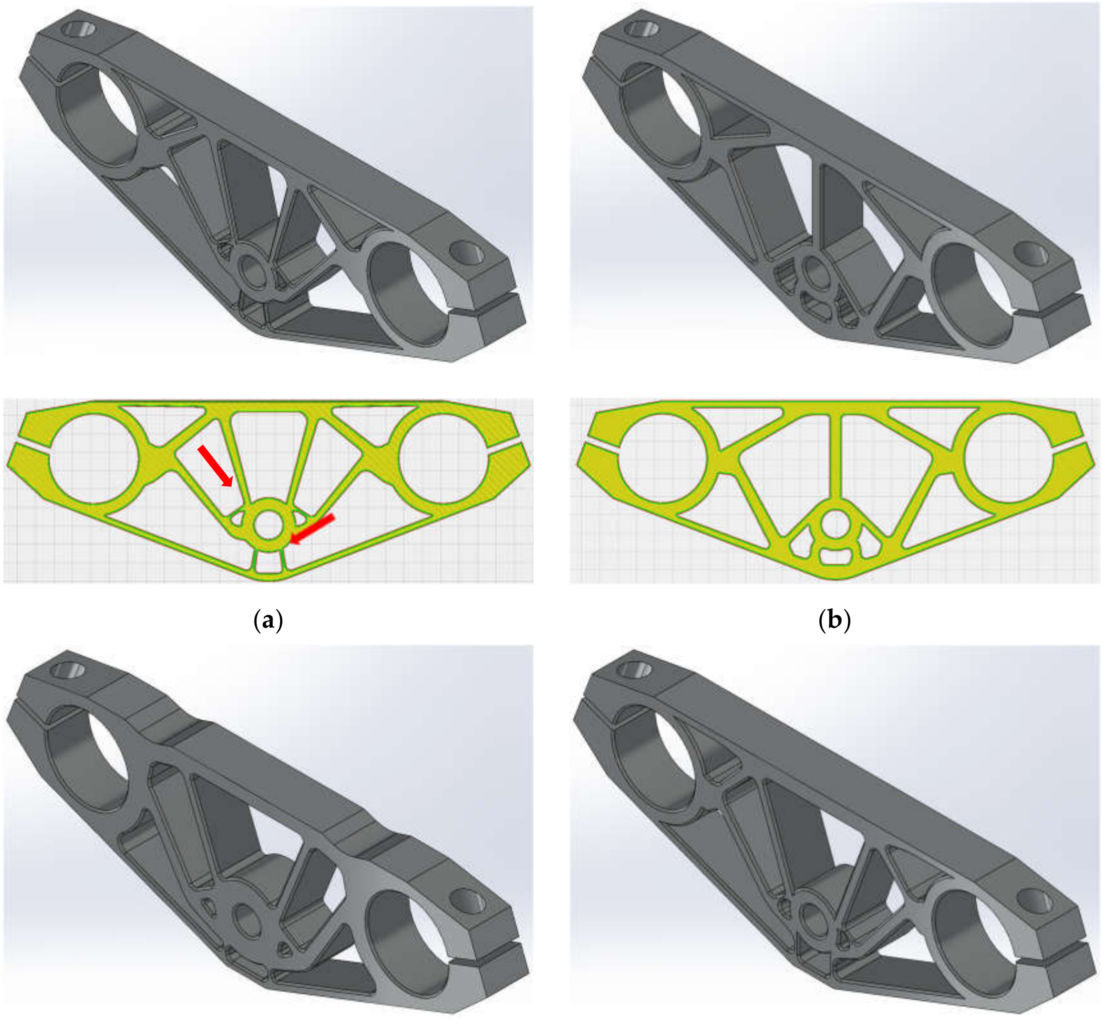

(**a**) (**b**)

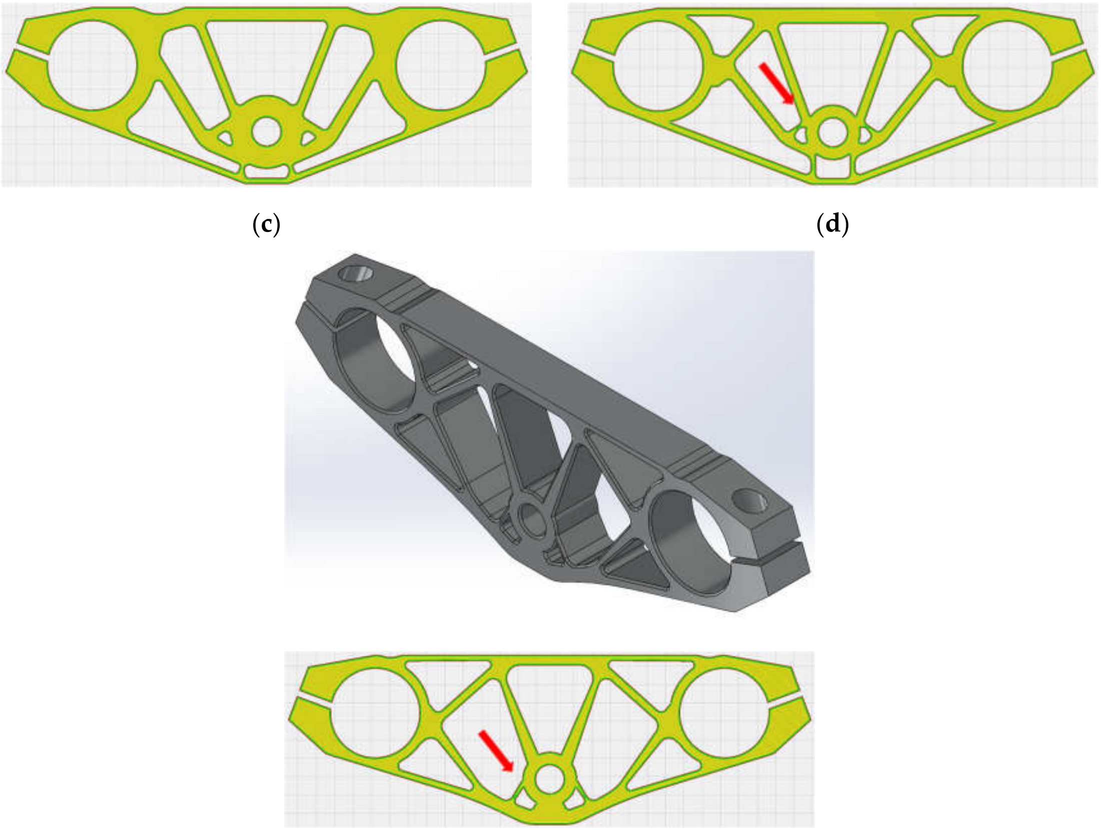

(c) (d)

(e)

Figure 6. CAD Interpretations and manufacturing analysis through Ultimaker Cura analysis of every optimization result. (**a**) HyperMesh 2023.1 CAD (**b**) CREO Parametric 6.0.1.0 (**c**) SolidWorks 2023. (**d**) ANSYS Workbench 2023 R1. (**e**) MATLAB. Pointed with red arrows, the critical features for checking the minimum length constraint.

All the interpretations satisfy the minimum length constraint, with the slicer computing a minimum of six solid perimetral layers. HyperMesh 2023.1 (**Error! Reference source not found.**a) and MATLAB implementations (**Error! Reference source not found.**e) are zoomed in for better clarity on the minimum length constraints. These critical features are highlighted with red circles in **Error! Reference source not found.**.

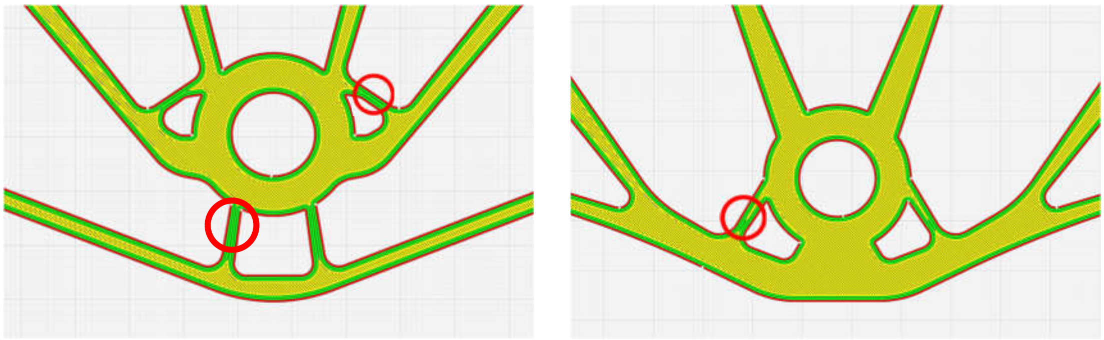

(a) (b)

Figure 7. Detail of the critical features for the minimum length constraint. (**a**) HyperMesh 2023.1 result. (**b**) MATLAB implementations result. Highlighted with red circles, the zones where the minimum length constraint is activated and only six solid perimetral layers are computed.

6. Conclusions

This paper presents an algorithm for updating the design variables of a topology optimization process. The algorithm is conceived to keep the final design space volume always under the target value at the time is possible to update the design variables and search for a valid design.

Additionally, a comparison of four commercial software packages with self-implementations in a MATLAB topology optimization code is carried out through the example of a racing motorcycle triple-tree. The aim was to illustrate the benefits of understanding the topology optimization process and having the ability to control the whole process, orienting it to a design case. Based on this, the following conclusions are drawn:

Commercial software packages offer a straightforward method for conducting topology optimization, but they fall short of yielding a quality density field for post-processing. As the software's resulting discreteness is poor, the latter CAD interpretation leads to a violation of the initial optimization constraints and, in the last term, a non-optimal design. Getting a low $\mathrm{M_{nd}}$ value ensures the interpretation is consistent with the optimization constraints.

The implementations presented in section 0 are effective. The geometry introduction through active and passive elements works correctly but it takes more time to introduce the geometry manually with formulas than introducing a CAD. Future implementations could introduce a macro for CAD parts introduction. The Heaviside step function written as a close-open filter achieves the desired minimum length scale, as demonstrated in section 0. The presented convergence algorithm has provided a result with low interpretability (this is a low $\mathrm{M_{nd}}$ value), leading to a CAD design interpretation in line with the optimization constraints.

In broader terms, the authors believe that the implementations developed in this study result in a more design-friendly algorithm for the optimization of real parts and can be easily implemented in the existing topology optimization processes.

Author Contributions: Conceptualization, A.V. and A.C.; methodology, A.V., J.M., A.B and A.C..; software, A.V..; validation A.V., J.M., A.B and A.C.; investigation, A.V. and A.C.; resources, C.C..; writing—original draft preparation, A.V., J.M. and A.B.; writing—review and editing, A.V., J.M. and A.B.; supervision, J.M., A.B and A.C.; project administration, C.C.; funding acquisition, C.C. All authors have read and agreed to the published version of the manuscript.

Funding: The research work described in this paper is part of the R&D and Innovation projects MC4.0 PID2020-116984RB-C21 and MC4.0 PID2020-116984RB-C22 supported by the MCIN/AEI/10.13039/501100011033.

Data Availability Statement: The original data presented in the study are openly available in Dropbox at https://www.dropbox.com/scl/fi/q436i732ldwzmuekxse0i/TijasPaperSym.m?rlkey=fgra5ae64nwvs2b3pgn2i3plm&st=t6ec8rdp&dl=0. Readers can also write the corresponding author (Abraham Vadillo Morillas - abvadill@ing.uc3m.es) for solving any question about the configuration of the code for obtaining different results.

Acknowledgments: The research work described in this paper is part of the R&D and Innovation projects MC4.0 PID2020-116984RB-C21 and MC4.0 PID2020-116984RB-C22 supported by the MCIN/AEI/10.13039/501100011033. Authors specially thank the Department of Industrial Engineering of the Alma Mater Studiorum Università di Bologna and their research group for allowing the collaboration and stay in their campus.

Conflicts of Interest: The authors declare no conflicts of interest.

References

1. Michell AGM (1904) LVIII. *The limits of economy of material in frame-structures*. The London, Edinburgh, and Dublin Philosophical Magazine and Journal of Science 8:589–597. https://doi.org/10.1080/14786440409463229
2. Schmit LA (1960) Structural design by systematic synthesis. In: 2nd Conference on Electronic Computation, ASCE. New York, pp 105–122
3. Dorn WS, Gomory RE, Greenberg HJ (1964) Automatic design of optimal structures. Journal de Mécanique 3:

4. Argyris JH (1954) Energy Theorems and Structural Analysis: A Generalized Discourse with Applications on Energy Principles of Structural Analysis Including the Effects of Temperature and Non-Linear Stress-Strain Relations. Aircraft Engineering and Aerospace Technology 26:347–356
5. Synge JL, Rheinboldt WC (1957) The hypercircle in mathematical physics. Phys Today 10:45–46
6. Clough RW (1960) The finite element in plane stress analysis. Proc 2^< nd> ASCE Confer On Electric Computation, 1960
7. Argyris JH (1965) Continua and discontinua, Matrix methods in structural mechanics, Opening address. In: Proceedings of the Conference held at Wright-Patterson Air Force Base, Ohio. pp 26–28
8. L. Logan D (2007) A first course in the finite element method. Thomson Canada Limited, Toronto
9. Cook RD (2007) Concepts and applications of finite element analysis, 1st ed. John Wiley & Sons
10. Bathe K-J (1996) Finite elements procedures in engineering analysis, 1st ed. Prentice-Hall Inc., Upper Saddle River, New Jersey
11. Park G-J (2007) Analytic methods for design practice. Springer Science & Business Media
12. Haftka RT, Gürdal Z (2012) Elements of structural optimization. Springer Science & Business Media
13. Bendsøe MP, Kikuchi N (1988) Generating optimal topologies in structural design using a homogenization method. Comput Methods Appl Mech Eng 71:197–224. https://doi.org/10.1016/0045-7825(88)90086-2
14. Sigmund O, Maute K (2013) Topology optimization approaches. Structural and Multidisciplinary Optimization 48:1031–1055. https://doi.org/10.1007/s00158-013-0978-6
15. Guest JK, Prévost JH, Belytschko T (2004) Achieving minimum length scale in topology optimization using nodal design variables and projection functions. Int J Numer Methods Eng 61:238–254. https://doi.org/10.1002/nme.1064
16. Andreassen E, Clausen A, Schevenels M, et al (2011) Efficient topology optimization in MATLAB using 88 lines of code. Structural and Multidisciplinary Optimization 43:1–16. https://doi.org/10.1007/s00158-010-0594-7
17. Liu K, Tovar A (2014) An efficient 3D topology optimization code written in Matlab. Structural and Multidisciplinary Optimization 50:1175–1196. https://doi.org/10.1007/s00158-014-1107-x
18. Schevenels M, Sigmund O (2016) On the implementation and effectiveness of morphological close-open and open-close filters for topology optimization. Structural and Multidisciplinary Optimization 54:15–21. https://doi.org/10.1007/s00158-015-1393-y
19. Pellens J, Lombaert G, Lazarov B, Schevenels M (2019) Combined length scale and overhang angle control in minimum compliance topology optimization for additive manufacturing. Structural and Multidisciplinary Optimization 59:2005–2022. https://doi.org/10.1007/s00158-018-2168-z
20. Langelaar M (2017) An additive manufacturing filter for topology optimization of print-ready designs. Structural and Multidisciplinary Optimization 55:871–883. https://doi.org/10.1007/s00158-016-1522-2
21. Langelaar M (2019) Topology optimization for multi-axis machining. Comput Methods Appl Mech Eng 351:226–252. https://doi.org/10.1016/j.cma.2019.03.037
22. Fu Y-F, Ghabraie K, Rolfe B, et al (2020) Smooth Design of 3D Self-Supporting Topologies Using Additive Manufacturing Filter and SEMDOT. Applied Sciences 11:238. https://doi.org/10.3390/app11010238
23. Lee HY, Zhu M, Guest JK (2022) Topology optimization considering multi-axis machining constraints using projection methods. Comput Methods Appl Mech Eng 390:. https://doi.org/10.1016/j.cma.2021.114464
24. Berrocal L, Fernández R, González S, et al (2019) Topology optimization and additive manufacturing for aerospace components. Progress in Additive Manufacturing 4:83–95. https://doi.org/10.1007/s40964-018-0061-3
25. Fritz C, Fischer L, Wund E, Zaeh MF (2023) Inner design of artificial test bones for biomechanical investigations using topology optimization. Progress in Additive Manufacturing 8:427–435. https://doi.org/10.1007/s40964-022-00343-1
26. Noordman B, Ton Y, van den Toorn J, et al (2023) Topology optimization for the design of a 3D-printed rotating shaft balance. Progress in Additive Manufacturing 8:19–25. https://doi.org/10.1007/s40964-022-00384-6
27. Zhu J, Zhou H, Wang C, et al (2020) A review of topology optimization for additive manufacturing: Status and challenges. Chinese Journal of Aeronautics 34:. https://doi.org/10.1016/j.cja.2020.09.020
28. Khadiri I, Zemzami M, Nguyen N-Q, et al (2023) Topology optimization methods for additive manufacturing: a review. International Journal for Simulation and Multidisciplinary Design Optimization Volume 14, 2023:12. https://doi.org/10.1051/smdo/2023015
29. Berce P (2024) Advances in Additive Manufacturing and Their Applications. Metals (Basel) 14:. https://doi.org/10.3390/met14020165
30. Prathyusha ALR, Raghu Babu G (2022) A review on additive manufacturing and topology optimization process for weight reduction studies in various industrial applications. Mater Today Proc 62:109–117. https://doi.org/https://doi.org/10.1016/j.matpr.2022.02.604

31. Choi W, Kim J, Park G-J (2016) Comparison study of some commercial structural optimization software systems. Structural and Multidisciplinary Optimization 54:685–699. https://doi.org/10.1007/s00158-016-1429-y
32. Dalpadulo E, Pini F, Leali F (2021) Assessment of Computer-Aided Design Tools for Topology Optimization of Additively Manufactured Automotive Components. Applied Sciences 11:10980. https://doi.org/10.3390/app112210980
33. Tyflopoulos E, Steinert M (2022) A Comparative Study of the Application of Different Commercial Software for Topology Optimization. Applied Sciences 12:611. https://doi.org/10.3390/app12020611
34. STRUZ J, HRUZIK L, KLAPETEK L, TROCHTA M (2023) COMPARATIVE ANALYSIS OF DIFFERENT SOFTWARES IN TERMS OF PARAMETERS OPTIMIZED BY TOPOLOGICAL OPTIMIZATION. MM Science Journal 2023:. https://doi.org/10.17973/MMSJ.2023_03_2022107
35. Sigmund O (2001) A 99 line topology optimization code written in Matlab. Structural and Multidisciplinary Optimization 21:120–127
36. Ferrari F, Sigmund O (2020) A new generation 99 line Matlab code for compliance topology optimization and its extension to 3D. Structural and Multidisciplinary Optimization 62:2211–2228. https://doi.org/10.1007/s00158-020-02629-w
37. Prager W (1968) OPTIMALITY CRITERIA IN STRUCTURAL DESIGN. Proceedings of the National Academy of Sciences 61:794–796. https://doi.org/10.1073/pnas.61.3.794
38. Karush W (2014) Minima of Functions of Several Variables with Inequalities as Side Conditions
39. Bruns TE, Tortorelli DA (2001) Topology optimization of non-linear elastic structures and compliant mechanisms. Comput Methods Appl Mech Eng 190:3443–3459. https://doi.org/10.1016/S0045-7825(00)00278-4
40. Bourdin B (2001) Filters in topology optimization. Int J Numer Methods Eng 50:2143–2158. https://doi.org/10.1002/nme.116
41. Sigmund O, Petersson J (1998) Numerical instabilities in topology optimization: A survey on procedures dealing with checkerboards, mesh-dependencies and local minima. Structural Optimization 16:68–75. https://doi.org/10.1007/BF01214002
42. Sigmund O (2007) Morphology-based black and white filters for topology optimization. Structural and Multidisciplinary Optimization 33:401–424. https://doi.org/10.1007/s00158-006-0087-x
43. Pratt WK (1991) Digital_Image_Processing, 1st ed. Wiley-Interscience, Michigan
44. Wang F, Lazarov BS, Sigmund O (2011) On projection methods, convergence and robust formulations in topology optimization. Structural and Multidisciplinary Optimization 43:767–784. https://doi.org/10.1007/s00158-010-0602-y
45. Driouch A (2020) Approximations based on the method of moving asymptotes. Université de Pau et des Pays de l'Adour; Université Ibn Tofail
46. Fernández E, Yang K, Koppen S, et al (2020) Imposing minimum and maximum member size, minimum cavity size, and minimum separation distance between solid members in topology optimization. Comput Methods Appl Mech Eng 368:113157. https://doi.org/https://doi.org/10.1016/j.cma.2020.113157
47. Trillet D, Duysinx P, Fernandez E (2021) Analytical relationships for imposing minimum length scale in the robust topology optimization formulation. Structural and Multidisciplinary Optimization 64:. https://doi.org/10.1007/s00158-021-02998-w
48. Wang F, Jensen J, Sigmund O (2011) Robust topology optimization of photonic crystal waveguides with tailored dispersion properties. JOSA B 28:387–397. https://doi.org/10.1364/JOSAB.28.000387
49. Jog CS (2001) A robust dual algorithm for topology design of structures in discrete variables. Int J Numer Methods Eng 50:1607–1618. https://doi.org/10.1002/nme.88
50. Zhang X, Takezawa A, Kang Z (2019) Robust topology optimization of vibrating structures considering random diffuse regions via a phase-field method. Comput Methods Appl Mech Eng 344:766–797. https://doi.org/https://doi.org/10.1016/j.cma.2018.09.022
51. PTC, Tonny Abbey (2021) PTC Creo Blogs. In: https://www.ptc.com/en/blogs/cad/topology-optimization-creates-rad-designs-how-to-make-sure-they-work
52. Thompson E (2023) Design Exploration via Topology Optimization. In: https://www.ansys.com/content/dam/amp/2023/october/quick-request/design-exploration-via-topology-optimization-et.pdf
53. Altair Engineering Inc. (2021) Practical Aspects of Structural Optimization, a Study Guide, 1st ed
54. Altair Engineering Inc. (2021) Altair OptiStruct Help Guide. In: https://2021.help.altair.com/2021/hwsolvers/os/topics/solvers/os/topology_opt_design_variables_r.htm
55. Dassault Systèmes (2021) SolidWorks Help Page. In: https://help.solidworks.com/2021/english/SolidWorks/cworks/c_simp_method_topology.htm

Disclaimer/Publisher's Note: The statements, opinions and data contained in all publications are solely those of the individual author(s) and contributor(s) and not of MDPI and/or the editor(s). MDPI and/or the editor(s) disclaim responsibility for any injury to people or property resulting from any ideas, methods, instructions or products referred to in the content.